

Two- and Three- View Geometry for Spherical Cameras

Akihiko Torii [†]

Atsushi Imiya ^{††}

Naoya Ohnishi [†]

[†] School of Science and Technology, Chiba University, Japan
{akit,ohnishi}@graduate.chiba-u.jp

^{††} Institute of Media and Information Technology, Chiba University, Japan
imiya@faculty.chiba-u.jp

Abstract

In this paper, we describe geometric aspects of two- and three-view geometry for spherical cameras. The geometric duality on a sphere leads us to re-consider geometric constraints for the three-dimensional reconstruction of points and lines. Using the geometric duality on a sphere, we derive geometric constraints, that is, epipolar circle constraint, for the three-dimensional reconstruction of points and lines.

1. Introduction

In this paper, we describe geometric aspects of two- and three-view geometry for spherical cameras. We first define the spherical camera model and derive the geometric duality of a point and a great circle on a sphere. Next, we formulate multiple-view geometry on spherical cameras, that is, epipolar geometry and trifocal tensor on the basis of spherical camera models. The geometric duality on a sphere leads us to re-consider geometric constraints for the three-dimensional reconstruction of points and lines. Finally, for the accurate and stable three-dimensional reconstruction of points and lines, we show the geometric constraints derived on the basis of multiple spherical camera geometry.

Catadioptric cameras are constructed by the combination of a pinhole camera and a quadric mirror [1, 2]. Dioptric cameras are constructed by the combination of pinhole camera and a fish-eye lens [3]. In this study, we call both catadioptric and dioptric cameras as omnidirectional cameras. The omnidirectional cameras are developed to capture a large field of view using a single camera device. The significant advantage of omnidirectional cameras is that it is possible to acquire a large field of view in a real time since motion of cameras and mosaicing are not required for the generation of omnidirectional images. These cameras are widely used in the robot navigation and video surveillance [4, 5, 6]. Recently, since omnidirectional camera systems are similar with the compound eyes of insects and fishes, the image analysis of omnidirectional vision systems is fo-

cused on biological vision community [7]. In the analysis of omnidirectional vision systems, a spherical camera is the essential camera model because all central catadioptric- and dioptric- cameras can be transformed to spherical cameras when the appropriate parameters of catadioptric and dioptric are known [8, 9].

For the achievement of camera network systems, which observe three-dimensional scenes and objects, it is essential task to employ different cameras, such as, conventional pinhole and omnidirectional cameras. For the mathematical and geometrical analysis of the camera network system, which uses a class of central cameras [9], the spherical camera model is the fundamental geometric expression because, geometrically, it is possible to transform the conventional pinhole and central omnidirectional cameras to spherical cameras. Therefore, it is necessary to clarify the multiple view geometry on spherical cameras for constructing the well-established camera network systems.

Multiple view geometry on pinhole cameras [10, 11] has been studied as a fundamental tool for three-dimensional scene reconstruction in the computer vision community. Pinhole camera models defined on the basis of projective geometry enable us to solve the problems on three-dimensional reconstruction lineally. The study of multiple view geometry on pinhole camera models clarifies that there exists geometric constraints for points and lines in a space up to four views. Multiple view geometry on spherical cameras has similar properties to one on pinhole cameras in the sense that algebraic representation. The significant difference is that spherical camera models clarify the geometric aspects of constraints among points, lines and camera positions on the basis of duality on a sphere. The formulation and analysis of multiple view geometry on spherical cameras are essential task to develop the vision systems for robots which use cameras as compound eyes.

2. Spherical Cameras

2.1. Spherical Camera Model

Definition 1 A central camera is a collection of rays, which pass through a single point in a space. The single point is a camera center.

Definition 2 A spherical camera model consists of a camera center and a surface of a unit sphere whose center is the camera center.

We call this surface of a unit sphere "spherical image" and the center of spherical surface "spherical camera center".

We formulate the relation between a point on a spherical image and a point in a space. As illustrated in Figure 1 (a), setting a spherical camera center $\mathbf{C} \in \mathbb{R}^3$ to be the origin of the world coordinate system, the spherical camera correct a ray from a point $\mathbf{X} \in \mathbb{R}^3$ to the camera center \mathbf{C} . The intersection of the ray and spherical surface yield a point $\mathbf{x} \in S^2$. We have the equation between \mathbf{x} and \mathbf{X} ,

$$\mathbf{x} = \frac{1}{|\mathbf{X}|} \mathbf{X}. \quad (1)$$

Since \mathbf{x} is a point on a unit sphere, it is possible to express in spherical coordinates, such that,

$$\mathbf{x} = \begin{pmatrix} x \\ y \\ z \end{pmatrix} = \begin{pmatrix} \cos \theta \sin \varphi \\ \sin \theta \sin \varphi \\ \cos \varphi \end{pmatrix}. \quad (2)$$

Therefore, the spherical image is expressed as $I_S(\theta, \varphi)$ where $0 \leq \theta < 2\pi$ and $0 \leq \varphi < \pi$.

Furthermore, as illustrated in Figure 1 (b), for a line L in a space, there exists a plane π which passes through a spherical camera center \mathbf{C} and the line L . The intersection of this plane π and the spherical surface yields a great circle l on the unit sphere. The normal vector $\mathbf{a} \in S^2$ of the plane π expresses the great circle on the spherical image.

2.2. Duality of A Point and A Line on A Unit Sphere

As illustrated in Figure 2 (a), since a great circle on the unit sphere $S^2 \in \mathbb{R}^3$ centered at the origin is the intersection of S^2 and a plane passing through the origin, a great circle defines a pair of anti-directional unit normal vectors. Furthermore, as illustrated in Figure 2 (b), the anti-directional unit normal vectors define the same plane that passes through the origin. Therefore, a great circle corresponds to a vector on the positive unit hemisphere, as illustrated in Figures 3

(a) and (b), which is defined as

$$\begin{aligned} S_+^0 &= [1], \\ S_+^1 &= \{\mathbf{s}^2\} \cup S^1 \cap H_+^2, \quad \mathbf{s}^2 = (s, 0)^\top, \quad s \in S_+^0, \\ H_+^2 &= \{(x, y) | y > 0\}, \\ S_+^2 &= \{\mathbf{s}^3\} \cup S^2 \cap H_+^3, \quad \mathbf{s}^3 = (S_+^1, 0)^\top, \\ H_+^3 &= \{(x, y, z) | z > 0\}. \end{aligned}$$

We set $\mathbf{x} \in \mathbb{R}^n$ and $\boldsymbol{\xi} \in \mathbb{P}^{n-1}$. For $\mathbf{n} \in S_+^2$ and $\mathbf{x} \in \mathbb{R}^3$, a great circle C is given as

$$C = \{\mathbf{x} | \mathbf{n}^\top \mathbf{x} = 0, |\mathbf{x}| = 1\}. \quad (3)$$

Therefore, formally the transformation from C to S_+^2 is expressed as

$$f(C) = \lambda \frac{\mathbf{x} \times \mathbf{y}}{|\mathbf{x} \times \mathbf{y}|}, \quad \mathbf{x}, \mathbf{y} \in S^2, \quad \lambda \in \{-1, 1\}, \quad (4)$$

$$f^{-1}(\mathbf{n}) = \{\mathbf{x} | \mathbf{n}^\top \mathbf{x} = 0, |\mathbf{x}| = 1, \mathbf{n} \in S_+^2\}, \quad (5)$$

where λ is selected so that vector $f(C)$ lies on S_+^2 . Equations (4) and (5) imply the duality of great circles and points on the sphere. The function $f(C)$ transforms points lying on a great circle to a point \mathbf{n} .

Furthermore, as illustrated in Figure 4, there exist correspondences between a line l on a plane and a point on S_+^2 ,

$$g(l) = \lambda \frac{\boldsymbol{\xi} \times \boldsymbol{\eta}}{|\boldsymbol{\xi} \times \boldsymbol{\eta}|}, \quad \boldsymbol{\xi} = (\mathbf{x}^\top, 1)^\top, \quad \boldsymbol{\eta} = (\mathbf{y}^\top, 1)^\top, \quad \mathbf{x}, \mathbf{y} \in l, \quad (6)$$

$$g^{-1}(\mathbf{n}) = \{\mathbf{x} | \mathbf{n}^\top \boldsymbol{\xi} = 0, \boldsymbol{\xi} = (\mathbf{x}^\top, 1)^\top, \mathbf{n} \in S_+^2\}. \quad (7)$$

The transformation is based on the embedding of projective plane P^2 to S^2 in \mathbb{R}^3 . Equations (6) and (7) imply the duality of a line on a plane and points on the sphere.

3. Two-View Geometry for Spherical Cameras

3.1. Epipolar Geometry for Spherical Cameras

Setting \mathbf{C} and \mathbf{C}' to be centers of spherical cameras, points $\mathbf{X} \in \mathbb{R}^3$ and $\mathbf{X}' \in \mathbb{R}^3$ are mapped to points \mathbf{x} and $\mathbf{x}' \in S^2$ on the spherical camera images as illustrated in Figure 5. We assume that $\mathbf{C} = \mathbf{0}$, and \mathbf{R} and \mathbf{t} express the transform of the camera coordinates between \mathbf{C} and \mathbf{C}' . The mapping are expressed as follows,

$$\lambda \mathbf{x} = \mathbf{X}, \quad \lambda \in \mathbb{R} \quad (8)$$

$$\lambda' \mathbf{x}' = \mathbf{X}' = \mathbf{R}\mathbf{X} + \mathbf{t}, \quad \lambda' \in \mathbb{R}. \quad (9)$$

Therefore, we have the equation,

$$\lambda' \mathbf{x}' - \lambda \mathbf{R}\mathbf{x} + \mathbf{t} = \mathbf{0}. \quad (10)$$

In the same manner of epipolar geometry on pinhole cameras [10, 11], since the vectors \mathbf{x}' , $R\mathbf{x}$ and \mathbf{t} are coplanar, we obtain the epipolar constraint for spherical cameras, that is,

$$\mathbf{x}'E\mathbf{x} = 0, \quad E = [\mathbf{t}]_{\times}R, \quad (11)$$

where $[\mathbf{t}]_{\times}$ is a skew-symmetric matrix. The 3×3 matrix E is linearly computed using eight pairs of corresponding points on the spherical images.

3.2. Epipolar Circle

The geometric duality of points and great circles on a sphere derives that points \mathbf{x} and $\mathbf{x}' \in S^2$ draw great circles l and l' , respectively. Since l and l' are on planes π and π' in \mathbb{R}^3 which pass through the centers of cameras \mathbf{C} and \mathbf{C}' , the intersection of these planes yields a line in \mathbb{R}^3 as illustrated in Figure 6 (a). We express this line as L ¹. Furthermore, we set the X_0 to be a point of intersection of the line L and the epipolar plane on which \mathbf{x} , \mathbf{x}' and \mathbf{X} are included. Since we select the points \mathbf{x} and \mathbf{x}' corresponding to the point \mathbf{X} , the six points X_0 , \mathbf{x} , \mathbf{x}' , \mathbf{C} , \mathbf{C}' and \mathbf{X} exist on the same epipolar plane as illustrated in Figure 6 (b). Moreover, since X_0 is the intersection of lines, which pass through \mathbf{C} and \mathbf{C}' and are perpendicular to \mathbf{x} and \mathbf{x}' , on the epipolar plane, the four points X_0 , \mathbf{C} , \mathbf{C}' and \mathbf{X} are on a circle on the epipolar plane as illustrated in Figure 6 (b). On the other hand, the convex polygon formed by these four points has a circumcircle. We call this circle as *epipolar circle*. This epipolar circle has a center $e_0 = \frac{1}{2}(\mathbf{X}_0 + \mathbf{X})$ and a radius $e_r = \frac{1}{2}|(\mathbf{X}_0 + \mathbf{X})|$. This epipolar circle leads the geometric aspect of trifocal tensor as described in Section 4.1.

The epipolar circle clarifies the relation of a point at infinity and the epipole. If \mathbf{X} is a point at infinity, X_0 is on the epipole, π and π' become an identical plane, and epipolar circle corresponds to the epipole. If X_0 is a point at infinity, \mathbf{X} is on the epipole, π and π' are parallel, and epipolar circle corresponds to the epipole.

4. Three-View Geometry for Spherical Cameras

4.1. Trifocal Tensor for Spherical Cameras

We express a line in a space by parametric form $L : X_I + \eta\mathbf{p} \in \mathbb{R}^3$ where $X_I \in \mathbb{R}^3$, $\mathbf{p} \in \mathbb{R}^3$ and $\eta \in \mathbb{R}$. Setting \mathbf{C} , \mathbf{C}' and \mathbf{C}'' to be centers of spherical cameras, lines L , L' and $L'' \in \mathbb{R}^3$ are mapped as great circles l , l' and $l'' \in S^2$ on the spherical camera images as illustrated in Figure 7. We assume that $\mathbf{C} = \mathbf{0}$ at the origin of world coordinates. R'

¹Notice that the direction vector of this line L corresponds to the normal vector of the epipolar plane. Therefore, we have the relation,

$$\mathbf{p} = \frac{\mathbf{x}' \times R\mathbf{x}}{|\mathbf{x}' \times R\mathbf{x}|} = \frac{\mathbf{t} \times R\mathbf{x}}{|\mathbf{t} \times R\mathbf{x}|} = \frac{\mathbf{x}' \times \mathbf{t}}{|\mathbf{x}' \times \mathbf{t}|}. \quad (12)$$

and \mathbf{t}' , and R'' and \mathbf{t}'' express the transforms of the camera coordinates among \mathbf{C} and \mathbf{C}' , and \mathbf{C} and \mathbf{C}'' , respectively.

According to the geometric duality between a great circle and a point on a sphere, the great circles l , l' and l'' equivalently denote points \mathbf{a} , \mathbf{a}' and $\mathbf{a}'' \in S^2$. It is possible to express the relations among the lines L , L' and L'' in a space and the points \mathbf{a} , \mathbf{a}' and \mathbf{a}'' on a sphere, such that,

$$\mathbf{a}^\top L = 0, \quad (13)$$

$$\mathbf{a}'^\top L' = \mathbf{a}'^\top (R'L + \mathbf{t}') = 0, \quad (14)$$

$$\mathbf{a}''^\top L'' = \mathbf{a}''^\top (R''L + \mathbf{t}'') = 0. \quad (15)$$

Using 3×4 matrix M , we can express these equations as the following form,

$$M\tilde{L} = 0, \quad (16)$$

where

$$M = \begin{bmatrix} \mathbf{a}^\top & 0 \\ \mathbf{a}'^\top R' & \mathbf{a}'^\top \mathbf{t}' \\ \mathbf{a}''^\top R'' & \mathbf{a}''^\top \mathbf{t}'' \end{bmatrix}, \quad (17)$$

and $\tilde{L}^\top = (L^\top, 1)^\top$. Since this equation implies a line in a space, $\text{rank}(M) = 2^2$. Setting $M^\top = (\mathbf{m}_1, \mathbf{m}_2, \mathbf{m}_3)$,

$$\mathbf{m}_1 = \alpha\mathbf{m}_2 + \beta\mathbf{m}_3. \quad (19)$$

Noting that $m_{14} = 0$, $\alpha = k\mathbf{t}''^\top \mathbf{a}''$ and $\beta = -k\mathbf{t}'^\top \mathbf{a}'$ where $k \in \mathbb{R}$. Again, in the same manner of trifocal tensor on pinhole cameras [10], we can express the relations among \mathbf{a} , \mathbf{a}' and \mathbf{a}'' using tensor notation, such that,

$$\mathbf{a} = \alpha R'^\top \mathbf{a}' + \beta R''^\top \mathbf{a}'' \quad (20)$$

$$= \mathbf{t}''^\top \mathbf{a}'' R_i'^\top \mathbf{a}' - \mathbf{t}'^\top \mathbf{a}' R_i''^\top \mathbf{a}'' \quad (21)$$

$$= \mathbf{a}''^\top (\mathbf{t}'' R_i'^\top) \mathbf{a}' - \mathbf{a}'^\top (\mathbf{t}' R_i''^\top) \mathbf{a}''. \quad (22)$$

For i th element of this vector,

$$a_i = \mathbf{a}''^\top (\mathbf{t}'' R_i'^\top) \mathbf{a}' - \mathbf{a}'^\top (\mathbf{t}' R_i''^\top) \mathbf{a}'' \quad (23)$$

$$= \mathbf{a}'^\top (R_i'^\top \mathbf{t}'') \mathbf{a}'' - \mathbf{a}''^\top (\mathbf{t}' R_i''^\top) \mathbf{a}', \quad (24)$$

where R_i' and R_i'' are the i th row vectors of R' and R'' . We have trifocal tensor $[T_1, T_2, T_3]$ which are the set of matrices $T_i = R_i'^\top \mathbf{t}'' - \mathbf{t}' R_i''^\top$. Rewriting Eqs. (20) and (23), we have the equations,

$$a_i = \mathbf{a}'^\top T_i \mathbf{a}'', \quad (25)$$

$$\mathbf{a}^\top = \mathbf{a}'^\top [T_1, T_2, T_3] \mathbf{a}''. \quad (26)$$

² $\text{rank}(M) = 2$ implies that the determinant of moment matrix of M equals to zero, that is, $|\mathbf{M}\mathbf{M}^\top| = 0$. We rewrite the matrix M as

$$M = \begin{bmatrix} \mathbf{a}^\top & \mathbf{0}_{1 \times 3} & \mathbf{0}_{1 \times 3} \\ \mathbf{0}_{1 \times 3} & \mathbf{a}'^\top & \mathbf{0}_{1 \times 3} \\ \mathbf{0}_{1 \times 3} & \mathbf{0}_{1 \times 3} & \mathbf{a}''^\top \end{bmatrix} \begin{bmatrix} I & \mathbf{0}_{3 \times 1} \\ R' & \mathbf{t}' \\ R'' & \mathbf{t}'' \end{bmatrix}. \quad (18)$$

Since a point \mathbf{x} on a great circle l satisfies

$$\mathbf{x}^\top \mathbf{l} = 0, \quad (27)$$

we have point-line-line correspondence, such that,

$$\mathbf{a}'^\top \left(\sum_i^3 x_i T_i \right) \mathbf{a}'' = 0. \quad (28)$$

Furthermore, setting \mathbf{x}' and \mathbf{y}' , and \mathbf{x}'' and \mathbf{y}'' to be the points on great circles l' and l'' , respectively, we have the relations,

$$\mathbf{a}' = k' \mathbf{x}' \times \mathbf{y}' = k' [\mathbf{x}']_{\times} \mathbf{y}', \quad (29)$$

$$\mathbf{a}'' = k'' \mathbf{x}'' \times \mathbf{y}'' = k'' [\mathbf{x}'']_{\times} \mathbf{y}'', \quad (30)$$

where k' and $k'' \in \mathbb{R}$ are selected so that \mathbf{a}' and \mathbf{a}'' are on S^2 . Eq. (28) is now represented as

$$\mathbf{a}'^\top \left(\sum x_i T_i \right) [\mathbf{x}'']_{\times} \mathbf{y}'' = 0, \quad (31)$$

$$\mathbf{y}''^\top [\mathbf{x}'''] \left(\sum x_i T_i \right) [\mathbf{x}''']_{\times} \mathbf{y}'' = 0. \quad (32)$$

Since \mathbf{x}' and \mathbf{x}'' are independent to \mathbf{y}' and \mathbf{y}'' , respectively, we have point-point-line and point-point-point correspondence as follows,

$$\mathbf{a}'^\top \left(\sum x_i T_i \right) [\mathbf{x}''']_{\times} = \mathbf{0}_{1 \times 3}, \quad (33)$$

$$[\mathbf{x}'''] \left(\sum x_i T_i \right) [\mathbf{x}''']_{\times} = \mathbf{0}_{3 \times 3}. \quad (34)$$

Noting that, for the derivations of point-point-line and point-point-point correspondence, homography is not used because homography among spherical cameras are not well-defined yet.

4.2. Geometric Aspect of Trifocal Tensor for Spherical Cameras

A triplet of corresponding points among spherical images yields three epipolar circles. In this section, we describe the epipolar circle constraint for the reconstruction of a point in a space.

For three cameras \mathbf{C}_a , \mathbf{C}_b and \mathbf{C}_c , setting \mathbf{x}_a , \mathbf{x}_b and $\mathbf{x}_c \in S^2$ to be a triplet of corresponding points to a point $\mathbf{X} \in \mathbb{R}^3$, respectively, there exist three epipolar planes π_{ab} , π_{bc} and π_{ca} as illustrated in Figure 8 (a). The duality of a point and a great circle on a sphere derives planes ξ_a , ξ_b and ξ_c for \mathbf{x}_a , \mathbf{x}_b and $\mathbf{x}_c \in S^2$. The intersections of ξ_a and ξ_b , ξ_b and ξ_c , and ξ_c and ξ_a yield lines \mathbf{L}_{ab} , \mathbf{L}_{bc} and $\mathbf{L}_{ca} \in \mathbb{R}^3$, respectively. Furthermore, we set \mathbf{X}_{ab} , \mathbf{X}_{bc} and \mathbf{X}_{ca} are the points of intersection of \mathbf{L}_{ab} and π_{ab} , \mathbf{L}_{bc} and π_{bc} , and \mathbf{L}_{ca} and π_{ca} .

For points \mathbf{C}_a , \mathbf{C}_b and \mathbf{X}_{ab} , \mathbf{C}_b , \mathbf{C}_c and \mathbf{X}_{bc} , and \mathbf{C}_c , \mathbf{C}_a and \mathbf{X}_{ca} , there exist three epipolar circles e_{ab} , e_{bc} and e_{ca} , respectively, as illustrated in Figure 8 (b). Obviously,

since we assumed a triplet of correct point correspondences, the three epipolar circles intersect a point \mathbf{X} in a space. If a triplet of point correspondences is not correct, the three epipolar circles do not meet at a point \mathbf{X} in a space. Therefore, this epipolar circle constraint enables us to search the corresponding points among spherical images accurately and stably. Furthermore, the computation of three-epipolar-circle intersection enables us to evaluate the accuracy of reconstructed points in a space and estimated camera positions, since the three epipolar circles should intersect at a single point in a space. Moreover, if the centers of three spherical camera lie on a line in a space, the three epipolar planes π_{ab} , π_{bc} and π_{ca} express the same plane in a space. It is not possible to reconstruct a point in a space using the intersection of these three epipolar planes. However, it is possible to reconstruct a point in a space using the intersection of three epipolar circles since there always exist three independent epipolar circles. This geometrical property leads to the conclusion that three-epipolar-circle intersection enables us to reconstruct points in a space for all geometric configuration of spherical cameras.

5. Discussions and Concluding Remarks

In this paper, we described geometric aspects of two- and three-view geometry for spherical cameras. Using geometric duality of a point and a great circle on a sphere, we derived geometric constraints, that is, epipolar circle constraint, for the three-dimensional reconstruction of points and lines. This is the first step of our study on multiple view geometry for spherical cameras. We proposed the possibility for generating additional constraints for three-dimensional reconstruction of points and lines using three spherical cameras.

For the next step of this study, we focus on the following three issues. First, since points on a unit sphere are unit vectors, the geometric computation for three-dimensional reconstruction using unit vectors proposed in [12] are mathematically equivalent for our two-view geometry for spherical cameras. It is necessary to clarify the detailed relations between them mathematically and geometrically. Next, since four-view and N-view geometry for pinhole cameras are formulated by the quadrilinear relations [10, 11] and the factorization method [13, 14]. We would like to formulate the four- and N- view geometry for spherical cameras. Finally, it is necessary to derive the critical configurations of camera positions and points in a space for multiple spherical-camera systems.

References

- [1] S. K. Nayar: Catadioptric omnidirectional camera. *CVPR '97*, pp. 482–488, 1997.
- [2] S. Baker and S. K. Nayar: A theory of catadioptric image formation. *ICCV '98*, pp. 35–42, 1998.
- [3] S. F. Ray: *Applied Photographic Optics : Lenses and Optical Systems for Photography, Film, Video, Electronic and Digital Imaging*. Focal Press, Oxford, 3rd edition, 2002.
- [4] J. Gaspar, N. Winters and J. Santos-Victor: Vision-based navigation and environmental representations with an omnidirectional camera. *IEEE Transactions on Robotics and Automation*, vol. 16, no. 6, pp. 890–898, 2000.
- [5] N. Winters, J. Gaspar, G. Lacey and J. Santos-Victor: Omni-directional vision for robot navigation. In *Proc. IEEE Workshop on Omnis00*, 2000.
- [6] S. Hrabar and G. S. Sukhatme. A comparison of two camera configurations for optic-flow based navigation of a UAV through urban canyons. In *Proc. IEEE/RSJ International Conference on Intelligent Robots and Systems*, pp. 2673–2680, September 2004.
- [7] M.O. Franz, J.S. Chahl and H.G. Krapp: Insect-inspired estimation of egomotion. *Neural Computation*, vol. 16, no. 11, pp. 2245–2260, 2004.
- [8] B. Mičušík and T. Pajdla: Para-catadioptric camera auto-calibration from epipolar geometry. In Ki-Sang Hong and Zhengyou Zhang, editors, In *Proc. ACCV*, vol. 2, pp. 748–753, Seoul, South Korea, January 2004.
- [9] P. Sturm and S. Ramalingam: A generic concept for camera calibration. In LNCS 3021-3024, In *Proc. ECCV*, vol. 2, pp. 1–13, Prague, Czech Republic, Springer, May 2004.
- [10] R. I. Hartley and A. Zisserman: *Multiple View Geometry in Computer Vision*. Second edition. Cambridge University Press, 2004.
- [11] O. Faugeras, Q.-T. Luong and T. Papadopoulou: *The Geometry of Multiple Images: The Laws That Govern The Formation of Images of A Scene and Some of Their Applications*. MIT Press, 2001.
- [12] K. Kanatani: *Geometric Computation for Machine Vision*. Oxford University Press, Oxford, U.K., 1993.
- [13] C. Tomasi and T. Kanade: Shape and motion from image streams under orthography: A factorization method. *International Journal of Computer Vision*, vol. 9, pp. 137–154, November 1992.
- [14] K. Kanatani and Y. Sugaya: Factorization without factorization: complete recipe. *Memoirs of the Faculty of Engineering, Okayama University*, vol. 38, Nos. 1 & 2, pp. 61–72, March 2004.

A. Appendix I

A.1. Epipolar Geometry for Pinhole Cameras

As illustrated in Figure 9, we set that \mathbf{C} and \mathbf{C}' are centers of pinhole cameras and \mathbf{X} is a point in \mathbb{R}^3 . We assume that $\mathbf{C} = \mathbf{0}$, and \mathbf{R} and \mathbf{t} express the transform of the camera coordinates between \mathbf{C} and \mathbf{C}' . Furthermore, we set that \mathbf{p} and \mathbf{p}' are the homogeneous expression of points on the images of pinhole cameras \mathbf{C} and \mathbf{C}' . Since the vectors \mathbf{p}' , $\mathbf{R}\mathbf{p}$ and \mathbf{t} are coplanar, we have the well-known epipolar constraint for pinhole cameras [10, 11], that is,

$$\mathbf{p}'^T \mathbf{E} \mathbf{p} = 0, \quad \mathbf{E} = [\mathbf{t}]_{\times} \mathbf{R}, \quad (35)$$

where $[\mathbf{t}]_{\times}$ is a skew-symmetric matrix. The 3×3 matrix \mathbf{E} is linearly computed using eight pairs of corresponding points on the pinhole camera images.

A.2. Epipolar Circle on Pinhole Cameras

The geometric duality of points and planes for pinhole cameras derives that points \mathbf{p} and $\mathbf{p}' \in \mathbb{P}^2$ express planes π and π' which pass through the camera centers \mathbf{C} and \mathbf{C}' , respectively and have normal vectors \mathbf{p} and \mathbf{p}' . The intersection of these planes yields a line $\mathbf{L} \in \mathbb{R}^3$ as illustrated in Figure 10 (a). In the same manner of epipolar circle on spherical cameras, we set the \mathbf{X}_0 to be a point of intersection of the line \mathbf{L} and the epipolar plane on which \mathbf{p}' , \mathbf{p} and \mathbf{X} exist. The six points \mathbf{X}_0 , \mathbf{p}' , \mathbf{p} , \mathbf{C} , \mathbf{C}' and \mathbf{X} are coplanar. Furthermore, the four points \mathbf{X}_0 , \mathbf{C} , \mathbf{C}' and \mathbf{X} are on a circle on the epipolar plane as illustrated in Figure 10 (b). On the other hand, the convex polygon formed by these four points has a circumcircle. This is the *epipolar circle*.

B. Appendix II

B.1. Trifocal Tensor for Pinhole Cameras

As illustrated in Figure 11, we set a line $\mathbf{L} \in \mathbb{R}^3$. Setting \mathbf{C} , \mathbf{C}' and \mathbf{C}'' to be centers of pinhole cameras, we assume that $\mathbf{C} = \mathbf{0}$ at the origin of world coordinates. \mathbf{R}' and \mathbf{t}' , and \mathbf{R}'' and \mathbf{t}'' express the transforms of the camera coordinates among \mathbf{C} and \mathbf{C}' , and \mathbf{C} and \mathbf{C}'' , respectively. Furthermore, we set that \mathbf{l} , \mathbf{l}' and \mathbf{l}'' are the homogeneous expression of lines on the images of pinhole cameras \mathbf{C} , \mathbf{C}' and \mathbf{C}'' . For

the triplets of lines on the pinhole camera images, we have the well-known trifocal tensor for pinhole cameras [10], that is,

$$l_i = \mathbf{l}'^\top T_i \mathbf{l}'', \quad (36)$$

$$\mathbf{l}'^\top = \mathbf{l}''^\top [T_1, T_2, T_3] \mathbf{l}'', \quad (37)$$

where $[T_1, T_2, T_3]$ are the set of matrices $T_i = R_i'^\top \mathbf{t}'' - \mathbf{t}' R_i''^\top$.

B.2. Geometric Aspect of Trifocal Tensor for Pinhole Cameras

For three pinhole cameras C_a, C_b and C_c , setting p_a, p_b and $p_c \in \mathbb{P}^2$ to be a triplet of corresponding points to a point $X \in \mathbb{R}^3$, respectively, there exist three epipolar planes π_{ab}, π_{bc} and π_{ca} as illustrated in Figure 12 (a). The geometric duality of points and planes for pinhole cameras derives that points p, p' and $p'' \in \mathbb{P}^2$ express planes π, π' and π'' which pass through the camera centers C, C' and C'' , respectively and have normal vectors p, p' and p'' .

In the same manner of epipolar circle constraint for spherical cameras, the intersections of ξ_a and ξ_b , ξ_b and ξ_c , and ξ_c and ξ_a yield lines L_{ab}, L_{bc} and $L_{ca} \in \mathbb{R}^3$, respectively. Furthermore, we set X_{ab}, X_{bc} and X_{ca} are the points of intersection of L_{ab} and π_{ab}, L_{bc} and π_{bc} , and L_{ca} and π_{ca} . For points C_a, C_b and X_{ab}, C_b, C_c and X_{bc} , and C_c, C_a and X_{ca} , there exist three epipolar circles e_{ab}, e_{bc} and e_{ca} , respectively, as illustrated in Figure 12 (b).

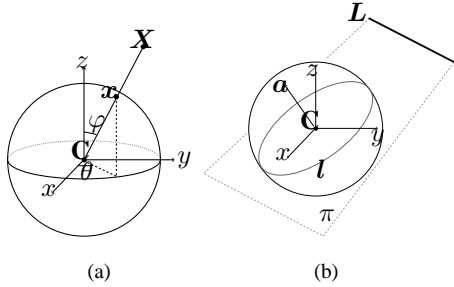


Figure 1: Spherical camera model. (a) The relation between a point in a space and a point on a spherical image. (b) The relation between a line in a space and a great circle on a spherical image.

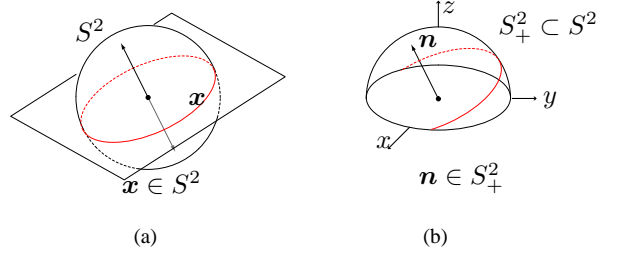


Figure 2: Duality of great circle and point on S^2_+ . As shown in (a), a great circle is the intersection of a sphere and a plane which passes through the origin. As shown in (b), the normal vector of this plane is an element in S^2_+ . This normal vector again defines a great circle on S^2_+ .

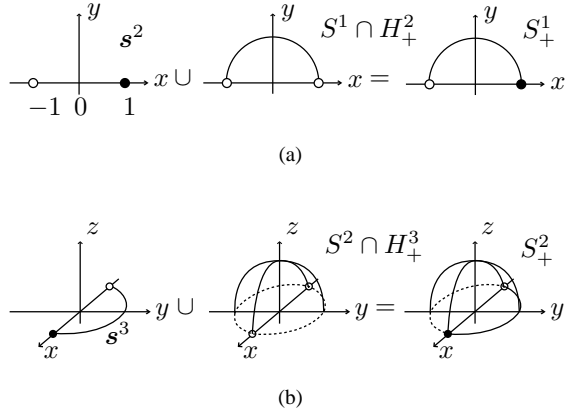


Figure 3: Diagram of definition of S^2_+ . (a) Definition of semicircle in \mathbb{R}^2 . (b) Definition of a positive hemisphere in \mathbb{R}^3 .

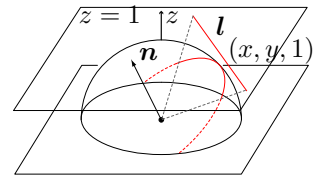


Figure 4: Duality of a line on a plane and a point on S^2_+ described in Eqs. (6) and (7). (a) A line on a plane tangent to the north pole of the unit sphere defines a normal vector of a plane which shows this line and the origin. This is a homogeneous expression of a line. The normal vector of this plane is an element of the positive hemisphere. This is a duality of line l and vector n .

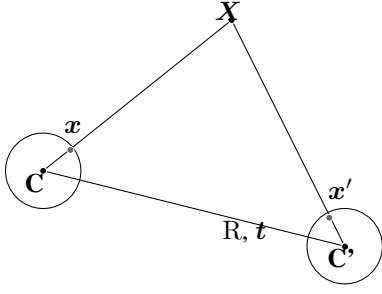


Figure 5: Epipolar geometry for spherical cameras. For a pair of points x and x' on spherical images, that correspond to a point in a space X , the points x , x' , X and the spherical camera centers C and C' are coplanar.

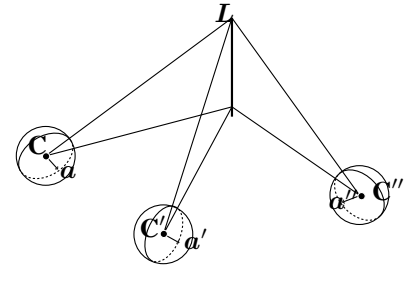


Figure 7: Three view geometry for spherical cameras. A line in a space is mapped as great circles on spherical images.

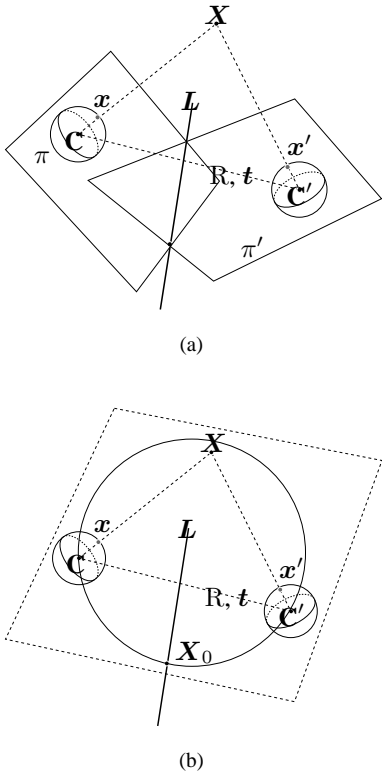


Figure 6: Epipolar circle for spherical cameras. (a) The geometric duality of points and great circles on a sphere derives that points x and $x' \in S^2$ draw great circles C and C' , respectively. The intersection of the planes π and π' , that include C and C' , yields a line in \mathbb{R}^3 . (b) The six points X_0 , x , x' , C , C' and X exist on the same epipolar plane. The four points X_0 , C , C' and X are on a circle on the epipolar plane.

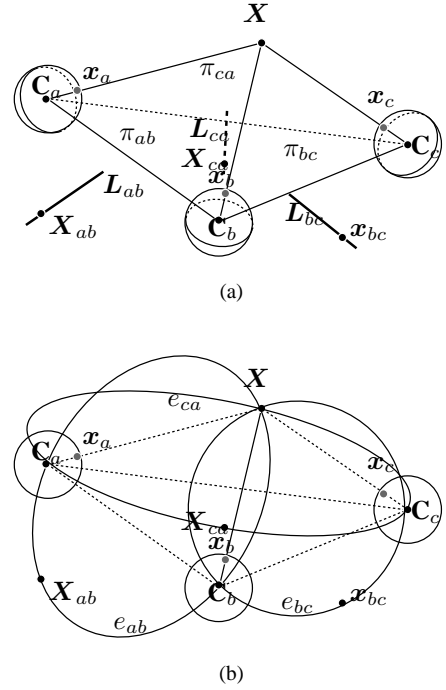


Figure 8: Epipolar circle constraint for spherical cameras. (a) For three cameras C_a , C_b and C_c , the triplet of points x_a , x_b and $x_c \in S^2$ corresponding to a point $X \in \mathbb{R}^3$ yields three epipolar planes π_{ab} , π_{bc} and π_{ca} . The intersections of ξ_a and ξ_b , ξ_b and ξ_c , and ξ_c and ξ_a yield lines L_{ab} , L_{bc} and $L_{ca} \in \mathbb{R}^3$, respectively. Furthermore, we set X_{ab} , X_{bc} and X_{ca} are the points of intersection of L_{ab} and π_{ab} , L_{bc} and π_{bc} , and L_{ca} and π_{ca} . (b) For points C_a , C_b and X_{ab} , C_b , C_c and X_{bc} , and C_c , C_a and X_{ca} , there exist three epipolar circles e_{ab} , e_{bc} and e_{ca} , respectively.

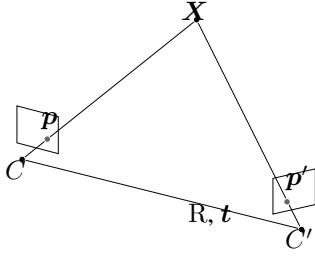


Figure 9: Epipolar geometry for pinhole cameras. For a pair of points p and p' on pinhole camera images, that correspond to a point in a space X , the points p , p' , X and the pinhole camera centers C and C' are coplanar.

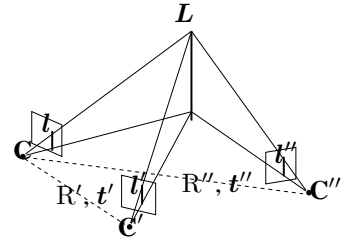
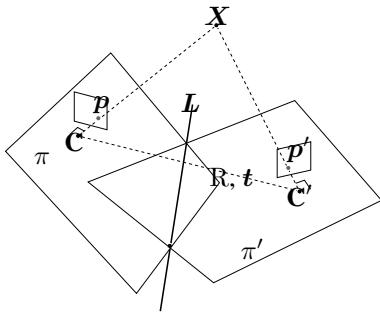
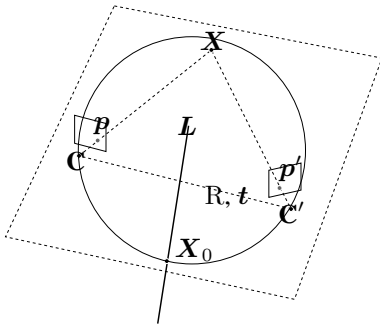


Figure 11: Three view geometry for pinhole cameras. A line in a space is mapped as lines on pinhole camera images.

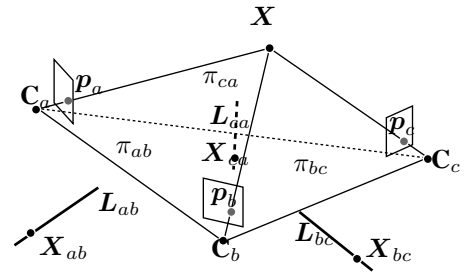


(a)

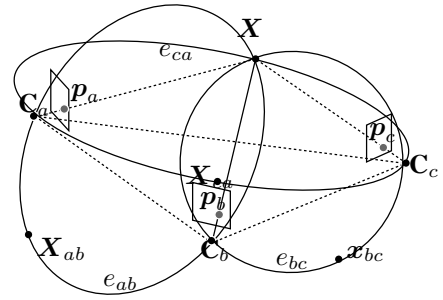


(b)

Figure 10: Epipolar circle for pinhole cameras. (a) The geometric duality of points and great circles on a sphere derives that points p and $p' \in S^2$ draw great circles C and C' , respectively. The intersection of the planes π and π' , that include C and C' , yields a line in \mathbb{R}^3 . (b) The six points X_0 , p , p' , C , C' and X exist on the same epipolar plane. The four points X_0 , C , C' and X are on a circle on the epipolar plane.



(a)



(b)

Figure 12: Epipolar circle constraint for pinhole cameras. (a) For three cameras C_a , C_b and C_c , the triplet of points p_a , p_b and $p_c \in S^2$ corresponding to a point $X \in \mathbb{R}^3$ yields three epipolar planes π_{ab} , π_{bc} and π_{ca} . The intersections of ξ_a and ξ_b , ξ_b and ξ_c , and ξ_c and ξ_a yield lines L_{ab} , L_{bc} and $L_{ca} \in \mathbb{R}^3$, respectively. Furthermore, we set X_{ab} , X_{bc} and X_{ca} are the points of intersection of L_{ab} and π_{ab} , L_{bc} and π_{bc} , and L_{ca} and π_{ca} . (b) For points C_a , C_b and X_{ab} , C_b , C_c and X_{bc} , and C_c , C_a and X_{ca} , there exist three epipolar circles e_{ab} , e_{bc} and e_{ca} , respectively.